



DOI: 10.5604/01.3001.0054.5685

# Broken engine's crankshaft misalignment inspection by using reverse engineering technique

W. Khuanlieng, S. Chuvaree, P. Janmanee \*

Department of Mechanical and Industrial Engineering, Faculty of Engineering, Rajamangala University of Technology Krungthep, Bangkok 10120, Thailand

\* Corresponding e-mail address: pichai.j@rmutk.ac.th

ORCID identifier:  <https://orcid.org/0000-0002-3239-4329> (P.J.)

## ABSTRACT

**Purpose:** The research aims to study the measuring data comparison between the broken crankshaft and the new crankshaft. The broken crankshaft has been investigated whether to measure dimensions or misalignment value. Therefore, the new crankshaft was measured and compared with a broken crankshaft using a 3D laser scanner. The misalignment value has been related to the overlapping value of a broken crankshaft by using a 3D software application.

**Design/methodology/approach:** The broken crankshaft has been compared with the new crankshaft in contemporary models. The broken crankshaft was produced and assembled from an automobile manufacturer's factory. It belonged to a particular Diesel engine that fractured while running in normal driving conditions. The broken crankshaft dimension has been investigated to find out the worn-out and misalignment value. The broken crankshaft inspection was measured using a micrometre and a 3D laser scanner application. Both crankshafts were created as artefact 3D models by the 3D laser scanner of the HandySCAN700 model. The accuracy of the 3D laser scanner will be presented in terms of measuring error. Two crankshafts were combined in concentric mate function. The inspection points were carried out at 4 points of each 90° around the main journal diameter, by following the guidelines of crankshaft inspection on a workshop manual basis. The overlapping value of each main journal will be measured by a 3D compare function at 0°, 90°, 180° and 270° respectively.

**Findings:** The results showed the average diameter of the broken crankshaft's main journal was less than the limit value. A new crankshaft was judged to be needed to be replaced. Moreover, it showed the lowest diameter of main journal No. 2 was 69.890 mm. It carried a 0.06% excessive worn-out value. The measuring error value of the 3D laser scanner was found and required for user-performed calibration procedures. The highest overlapping value was higher than the standard tolerance, up to 117%. It was located at the main journal No. 3 at 180° and near the fractured point of the broken crankshaft.

**Research limitations/implications:** The study of the broken crankshaft inspection was limited to either under-warranty or over-warranty cases. Most of the technicians in authorised automobile dealerships had no intention of performing the inspection process completely. In addition, they were lack of measuring skills and data records. Moreover, automotive manufacturers cannot support the 3D dimension data because it may affect the business's confidential data leakage.



**Practical implications:** The workshop manual mentioned the crankshaft inspection as a basic tool. In the case of complex components, automotive manufacturers should consider the utilisation of non-contact measuring tools for inspection reference.

**Originality/value:** A reverse engineering technique was applied to scan the broken crankshaft into a 3D model using 3D laser scanning technology, which is used to reduce the measuring time and measuring value error in the inspection process.

**Keywords:** Reverse engineering, Broken crankshaft, 3D laser scanner application, Crankshaft misalignment

**Reference to this paper should be given in the following way:**

W. Khuanlieng, S. Chuvaree, P. Janmanee, Broken engine's crankshaft misalignment inspection by using reverse engineering technique, Archives of Materials Science and Engineering 125/2 (2024) 65-74. DOI: <https://doi.org/10.5604/01.3001.0054.5685>

## METHODOLOGY OF RESEARCH, ANALYSIS AND MODELLING

### 1. Introduction

Nowadays, several automotive industry sectors require substantially more precise technologies than those made in the past. The automobile, army and aerospace industries are exclusively concerned with product inspection and combustion engine systems [1,2]; the crankshaft is the most important part. Almost all crankshafts are produced of either forged steel or cast iron by the manufacturers. They have a complex geometry design. A crankshaft is a mechanical component that is assembled with a piston and connecting rod. The combustion power will be converted from reciprocating motion into rotational motion [3,4].

The cause of the main bearing failure was misalignment that occurred with deviations from the concentricity of the crankcase housings [5,6]. The effects of misalignment on lubricating characteristics were examined because misalignment was frequently occurring under excessive load. In addition, when a main journal misaligns, the oil film cannot protect the journal-bearing shell, which causes high friction and deformation [7,8]. Research and development in the automotive industry were required to redesign the crankshaft to be equipped with the new engine generation, including hybrid technology [9].

Several pieces of literature offer methods concerning failure analysis and the redesign of a crankshaft. The impact of operating load and thermodynamic instability were studied in terms of metal structure elements that were inevitably manufactured, leading to fatigue failure. They greatly accelerate wear processes, exacerbate surface roughness, and reduce the fatigue strength of metal materials [10]. Failed parts required adequate technical analysis, such as consideration of operating conditions, climatic region conditions, season, and vehicle model. There were many parts that often relatively failed more than others that, according to their

reliability, were critical by significant evidence [11]. However, most investigations are frequently time-consuming and expensive, and they require a high level of expertise in the automotive field [12].

Portable 3D scanning devices have been used more frequently in a variety of applications. Most of these 3D scanning devices' typical application areas were restricted depending on the measuring object, including close-range, measuring techniques, and image-based and structured light systems. However, considering a 3D scanning system that was appropriate for a specific application. They were used to improve the models and to enhance the surface models' mesh quality [13]. In order to contribute to understanding, evaluating, and assessing the spectrum of potential applications for these portable measurement devices. Kersten et al. have already published comparative investigations on the geometrical accuracy of different hand-held 3D scanning systems. The research investigated quality by geometrical accuracy tests of the Creaform HandySCAN700 model. The quality of the measuring system was confirmed as a reference system with acceptable accuracy. It has demonstrated the ability to be of high quality and an excellent reference device [14].

Each type of Geomagic software package is specialized to support specific industry applications. The latest Geomagic Control X software is the ultimate metrology software for repeatable development and reliable quality inspection of manufacturing workflow [15]. Using non-contact scanners, measurements can be quickly taken on objects to make analyses and reports. Before going to the output, the post-processing software is required to be converted into a 3D file software application. Then, the manufacturing cycle processed the data into useable form, whether for 3D visualisation, reverse engineering, rapid prototyping, CNC machining or quality inspection, as workflow has been shown in Figure 1.

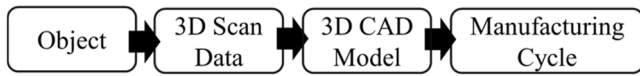


Fig. 1. Reverse engineering process workflow

The Vxelements software is a powerful integrated 3D software platform that fully synchronizes with 3D measuring and scanning technologies. While effective, most contact-based techniques of conventional measurement take a long time to create an accurate 3D model and can be efficient in measuring results. Non-contact-based techniques are implemented to get beyond contact-based limitations, which are required to control the relationship of light with an object [16]. Furthermore, choosing an appropriate tool for 3D measurement acquisition can prevent errors from accumulating throughout the design and production process [17]. The finalized version should be confirmed perfectly with the scanning data and actual inspection. As a result, accuracy validation is required to ensure the quality of reverse engineering [18]. In the previous work, the broken crankshaft has already been investigated and reported, including preliminary examination and failure mechanism observation, as shown in Figure 2 [19].

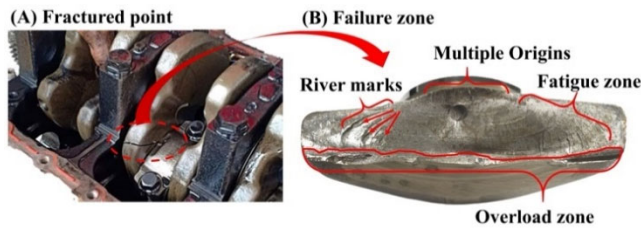


Fig. 2. Case study of the broken crankshaft; (A) the fractured point location; (B) cross section area of failure zone

However, there is still no dimensional investigation of misalignment inspection using reverse engineering techniques. Meanwhile, most crankshafts could not be inspected for misalignment after fracture. Therefore, the research has applied advanced measuring tools to look after the quality of products in the automotive aftersales market.

## 2. Methodology

### 2.1. Crankshaft model

Authorized automotive manufacturers produced two interesting crankshafts. The broken crankshaft was removed from an engine after 470,000 km. In addition, the cracked

position was in Crankpin No. 2 after the disassembled process. The crankshaft was separated into two parts, and it was impossible to reconnect as the original one. Moreover, the crankshaft runout inspection cannot be measured by uncompleted parts. The technical nomenclature of the crankshaft and fractured position are shown in Figure 3.

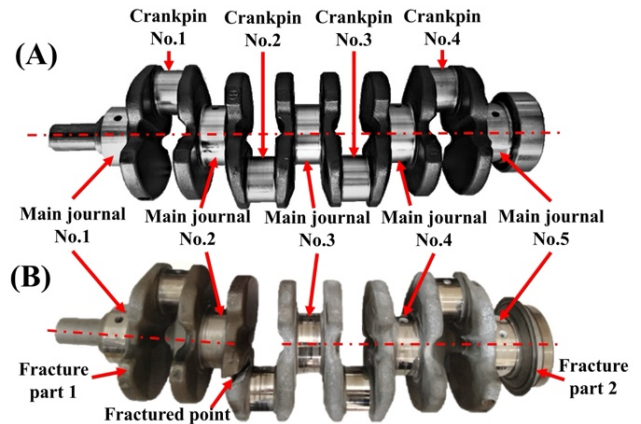


Fig. 3. Crankshaft nomenclature; (A) the new crankshaft; (B) the broken crankshaft and fractured position

Another new crankshaft was brought from a genuine spare parts shop, which would be the reference crankshaft for this research [20]. The model and specification of the engine are presented in Table 1.

Table 1. 4JJ1 engine specification

Type	Inline 4 – cylinder
Injection system	Common rail direct injection
Bore x stroke	95.4 mm × 104.9 mm
Displacement	2.999 L
Max power at 2,500 rpm	61 kW.
Max torque at 1,800 rpm	280 Nm
Weight	25.5 kg

### 2.2. 3D laser scanner

The HandySCAN700 model was a 3D laser scanner that was being utilized. It sets itself relative to detect objects with reference targets. Table 2 provides more details regarding the manufacturer's specifications for the 3D laser scanner [21].

Depending on the 3D laser scanner's performance, the main journal diameter size of the scan data could be oversized or undersized from the actual one. The measured value of the main journal diameter size of each journal as measured by a 3D laser scanner,  $d_{scan}$ , and the main journal diameter size of each journal as measured by a measuring

tool,  $d_{ref}$ , then the measuring error,  $C_S$ , as shown in equation (1) [22].

$$C_S = d_{scan} - d_{ref} \quad (1)$$

Table 2.

3D laser scanner specifications are given by the manufacturer

Specification	Value
Accuracy	Up to 0.030 mm
Measurement rate	480,000 Measurements/s
Measurement resolution	0.050 mm
Mesh resolution	0.200 mm
Scanning area	275 x 250 mm
Stand-off distance	300 mm
Depth of field	250 mm
Part size range	0.1-4 m
Software	VXelements

The 3D laser scanner's performance has been determined using the measuring error  $C_S$ . It represented a single figure of an average value for applying calculation in the research.

### 2.3. Experiments

The experiment described the steps to gather the required data. Figure 4 describes the dataset sequentially measured in the procedure as follows.

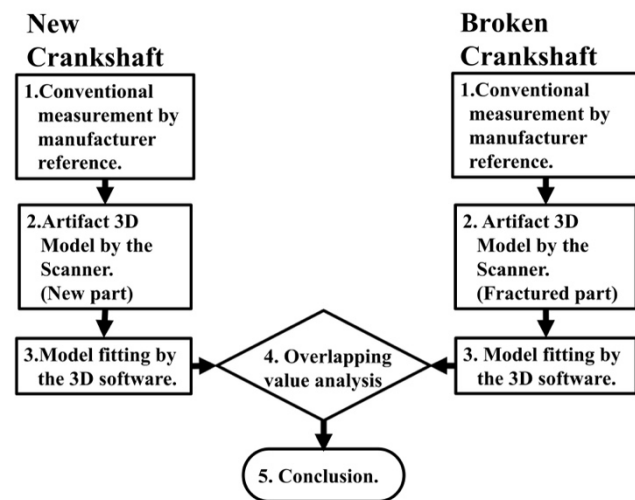


Fig. 4. Measuring procedure workflow

To determine the main journal diameter of the broken crankshaft and the new one.

They were measured by a micrometre. The measurement was carried out at least 4 points around the main journal diameter [23]. The position points are illustrated in Figure 5.

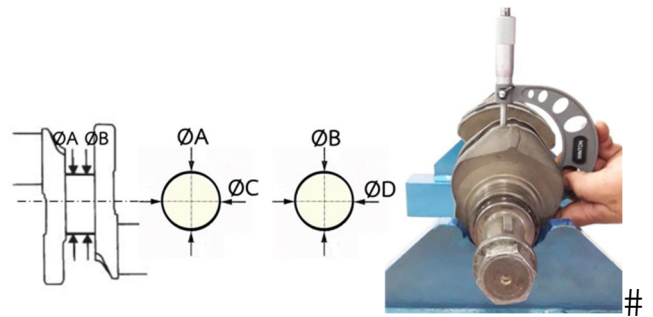


Fig. 5. Measuring position points of main journal diameter were inspected by micrometer

To remove oil stains from the crankshaft surface.

Two crankshafts were sprayed with color-checking powder (Developer) on all the components. The point markers were placed as reference points on the surface of the crankshafts and the surrounding area, see Figure 6.

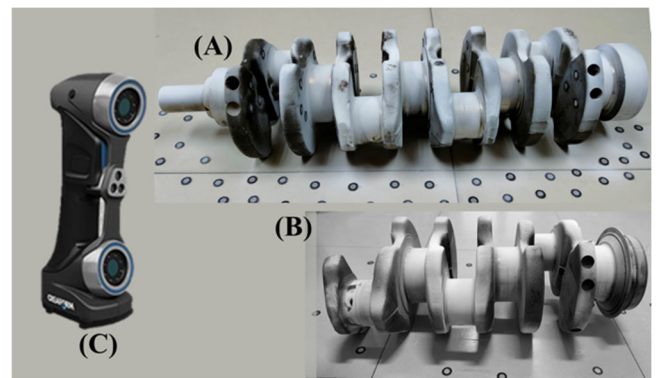


Fig. 6. (A) New crankshaft, (B) broken crankshaft, (C) 3D laser scanner

VXelement software is utilized to create an artefact 3D model processed with a 3D laser scanner and 3D modelling software.

All mesh has been generated automatically as a reference of the features. All data-based calculations were performed for precisely position-specific geometry.

During the 3D scanning process, a 3D laser scanner can detect at least three markers simultaneously. To ensure a 3D laser scanner gripping perpendicular to the surface. An operator must manually place the 3D laser scanner in all circumstances, as shown in Figure 7 [24].

VXelement software was equipped with the complementary tools feature, mesh optimisation, and smooth integration into the scan-based design, as shown in Figure 8. Moreover, CAD software is already available for drawing dimensions and 3D modelling capabilities.



Fig. 7. The new crankshaft was created to artefact a 3D model by a 3D laser scanner

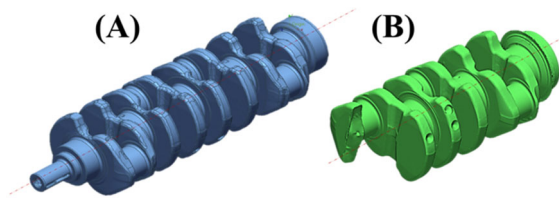


Fig. 8. (A) Artifact 3D model of the new crankshaft, (B) artifact 3D Model of the broken crankshaft

All scanning data was transferred to Geomagic Control X software.

The two crankshafts were combined by concentric mate function. Following the guidelines of crankshaft inspection on a workshop manual guideline basis, the inspection points were carried out at 4 points of each 90° around the main journal diameter. They were applied to measure at 0°, 90°, 180° and 270° respectively, by a 3D compare function. The function was performed with overlapping values when different value points happened. The highest value and position point of each main journal are significantly presented and related to the misalignment of a broken crankshaft. However, the broken crankshaft could not return the main journals No. 1 and No. 2 to the original part. Therefore, their measuring values were skipped in the 3D model inspection.

### 3. Results and discussion

The most significant dimension results have been investigated and are discussed below.

#### 3.1. Worn-out inspection of the main journal diameters

A micrometre was used to measure the main journal diameters. By comparing it with standard data, the allowed minimum size of the main journal diameter was 69.910 mm.

The runout inspection value of the crankshaft must not be more than 0.08 mm. Any measured values exceeding the standard must be replaced with a new crankshaft instead. The crankshaft specification size of the main journal is shown in Table 3. It was referred to from the manufacturer's workshop manual [23].

Table 3.

The specification data of the main journal crankshaft is in the workshop manual

Crankshaft main journal	Diameter size, mm
Maximum	69.932
Limit	≤ 69.910

The measured value of the broken crankshaft is shown in Table 4. The worn-out value of each main crankshaft journal can be identified. Following the worn-out value of each main journal, the lowest measured value of the main journal diameter No. 2 was 69.890 mm. It was less than the limited value of 69.910 mm. Therefore, a new crankshaft was required to be replaced after inspection.

To determine the worn-out value of each main journal diameter that, it is shown in Figure 9.

Table 4.

The main journal diameter measurement of the broken crankshaft

Main journal	φ A	φ B	φ C	φ D
No. 1	69.910	69.910	69.920	69.920
No. 2	69.890	69.910	69.900	69.910
No. 3	69.920	69.920	69.910	69.920
No. 4	69.920	69.920	69.920	69.920
No. 5	69.930	69.930	69.930	69.930

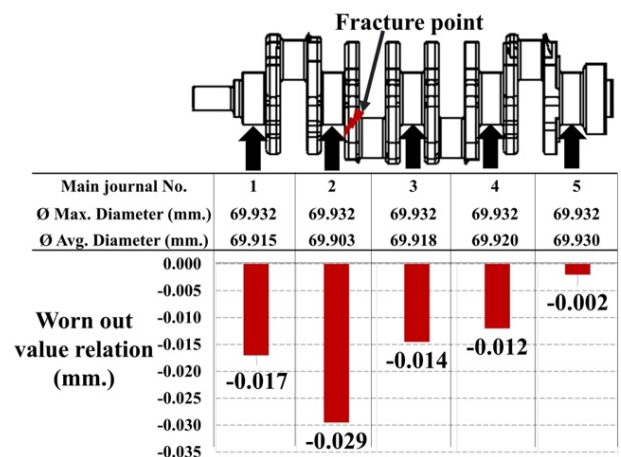


Fig. 9. Main journal diameter worn-out inspection of the broken crankshaft

Figure 9 presented the main journal diameter of the broken crankshaft. The measured value was compared with a maximum value when it was a new one. The actual worn-out value of average main journal diameter No. 5 was - 0.002 mm, which is the lowest worn-out rate. However, the actual worn-out value of average main journal diameter No. 2 was -0.029 mm, which is the highest worn-out rate. Considering the wear process, the material loss occurred due to the worn-out value relation of each main journal. The cross section area was changed by contact stress distribution while the crankshaft rotated. If the stress concentrations interfere with local concentrations of contact stresses, the surface coating may be damaged, and the wear resistance may deteriorate. Another parameter was the lubricating properties of the engine oil. If the viscosity accumulates impurities, they can act as an abrasive.[25] Generally, for the crankshaft in similar situations, all main journal diameters should be worn# closely to each other. In the case of the main journal, diameter No. 2 was immensely#worn out more than others. It was concerned with quality control on surface hardening in the heat treatment process. In addition, the worn-out value will be increased, and the clearance gap of the main journal-bearing shell will be expanded, which can lead to a misalignment of the crankshaft [26].

### 3.2. The measuring value comparison between 3D laser scanner and conventional measurement

The 3D geometrical model of the new crankshaft was created using VXElements software, shown in Figure 10.

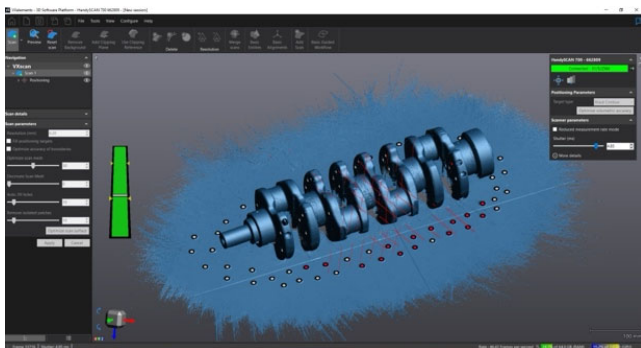


Fig. 10 The 3D model of the new crankshaft was created by VXElements software

The VXElements software has the capacity to produce 3D data in standard formats for any CAD platform. Both main journal diameter dimensions were measured by CAD software and a micrometre, as shown in Figure 11. The accuracy of scan data must be compared with the actual

measuring tool. The average main journal diameter of an artefact 3D model,  $d_{scan}$  was 70.000 mm. by a 3D laser scanner. Meanwhile, the average main journal diameter of an actual part,  $d_{ref}$  was 69.930 mm by a micrometer. Therefore, the measuring error,  $C_s$ , was calculated from  $70.000 - 69.930$  to be 0.070 mm. The results showed a measuring error over the accuracy limit of 0.030 mm. (Refer to data in Table 2). The technical specifications from HandySCAN700 are required for user-performed calibration procedures [27].

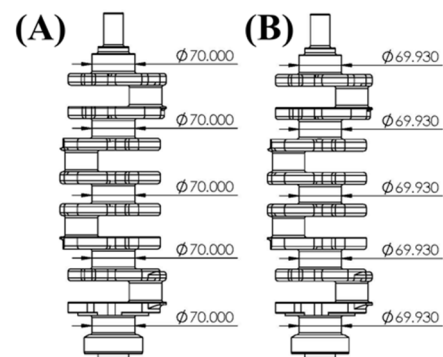


Fig. 11. (A) Main journal diameters were measured by a 3D laser scanner, and (B) main journal diameters were measured by a micrometre

### 3.3. Main journal overlapping value measurement

Even in unexpected locations, wear and deformation have constantly been visible. The automated alignment and deviation features analysis can locate and measure specific points, as shown in Figure 12. The artefact 3D model of a new crankshaft was set as the reference. Consequently, the 3D new crankshaft and the 3D broken crankshaft are combined in concentric mate function to measure the overlapping value. It is illustrated in Figure 13.

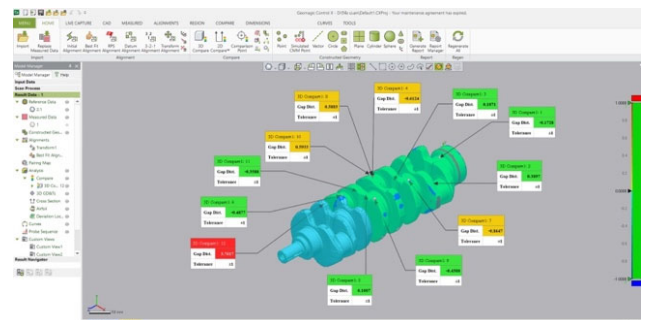


Fig. 12. The overlapping value was measured by Geomagic Control X software

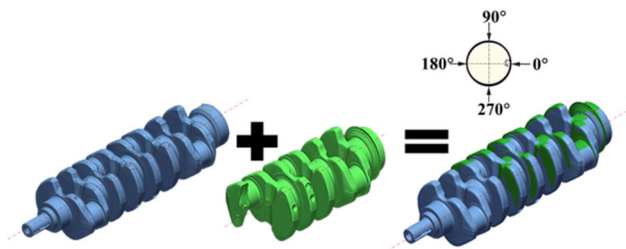


Fig. 13. The two 3D crankshafts are combined in concentric mate function for overlapping measurement

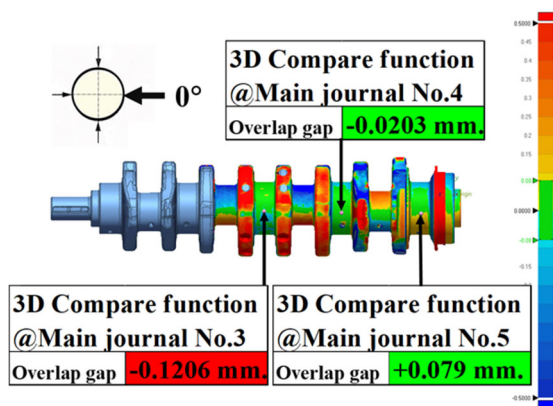


Fig. 14. The overlapping value measurement of the main journal at 0°

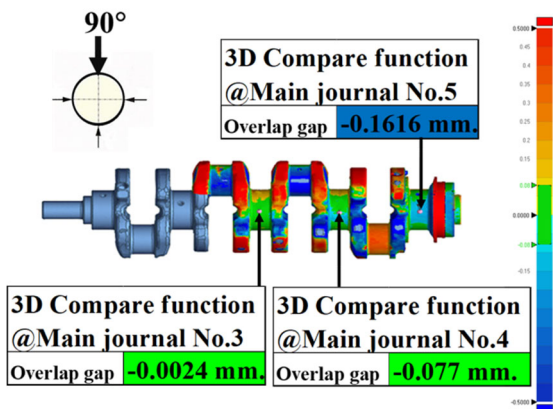


Fig. 15. The overlapping value measurement of the main journal at 90°

The 3D compare function shows the overlapping value of each main journal at 0° (Fig. 14). The overlapping value between two crankshafts is presented by observing visible colour with gap values. The range of green shade colour presented the overlap within an acceptable tolerance of

0.08 mm. The range of red shade colour presented the overlap over acceptable tolerance into a positive value. The positive value means the broken crankshaft surface over the reference surface. On the other hand, the range of blue shade colour presented the overlap over acceptable tolerance into a negative value. Also, the negative value means the broken crankshaft surface under the reference surface. Moreover, 3D compare functions have shown the measured value of each main journal at 90°, 180° and 270° respectively, in Figures 15-17.

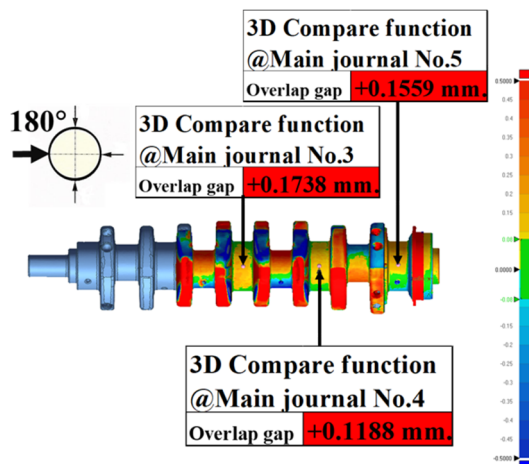


Fig. 16. The overlapping value measurement of the main journal at 180°

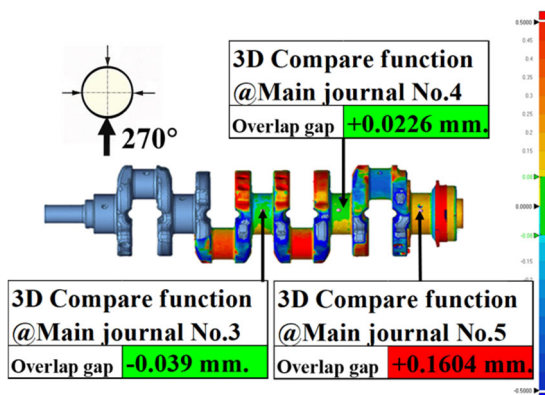


Fig. 17 The overlapping value measurement of the main journal at 270°

The measured value of the overlap seemed to be complicated in all 3D combined crankshafts. As a result, the overlapping value of main journal No. 3 at 180° was 0.1738 mm. which was the highest value in positive value. In addition, the main journals No. 4 and No. 5 at 180° also

presented the overlapping value on the positive value with significance. On the other hand, all overlapping values at 0° and 90° are almost negative values. The overlapping values are plotted using a Cartesian coordinate plane on the main journal diameter reference, as shown in Figure 18.

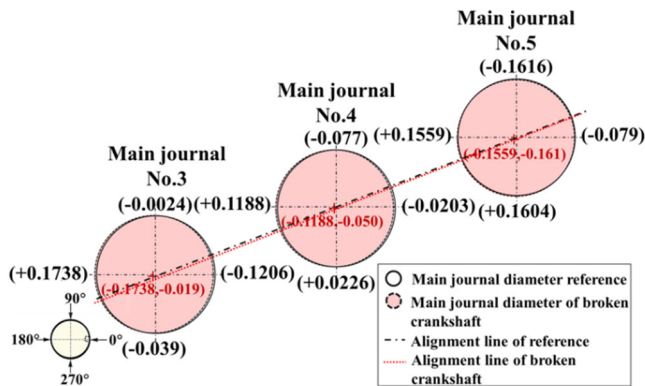


Fig. 18 The overlapping values of the 3D combined crankshafts

Most crankshaft failures were usually related to misalignment issues. Meanwhile, they were under high bending or torsion moment [28]. Forecasting during engine operation, the unexpected bending stress will be affected in the critical zone of the crankshaft, where the crack can easily initiate [29,30]. The initial crack gradually increased depending on engine load operation. It was obvious in the highest overlapping value, which was consistent with the fractured position of the crankshaft.

#### 4. Conclusions

It is an interesting broken crankshaft after cracking in normal driving conditions that was required to be compared with the new crankshaft for investigation. The study measured the broken crankshaft inspection using a micrometre and a 3D scanner application. The measured value using a micrometre of the main journal diameter No. 2 was 69.890 mm, compared with the maximum main journal diameter of 69.932 mm. Therefore, it showed a significant 0.06% maximum excessive worn-out value. Therefore, it may be reflected in the main journal No.2 about quality control on surface hardening in the heat treatment process. The misalignment value cannot be checked after the crankshaft is broken. A 3D scanner application was utilized using the overlapping measuring method instead. The measuring result of the highest different overlapping value was 0.1738 mm. It was higher than the standard tolerance, up to 117%. It was located at the main journal No. 3 at 180°

and also near the fractured point at crankpin No. 2. The overlapping measurement can be referred to as the misalignment of the broken crankshaft. In the given contribution, misalignment inspection results were achieved using a 3D model of reverse engineering technique. It approached complicated part measurement, including using crankshafts after long-term service operations or under engine overhaul inspection by automotive manufacturers and after-sales service markets.

The future scope of this research includes conducting a more in-depth failure fracture analysis of the transition fillet roughness. Additionally, the finite element analysis can be performed on the 3D model of the crankshafts to gain insights into their structural behaviour and operating performance.

#### Acknowledgements

The work was completed while the first author was a Doctoral Candidate in the Mechanical and Industrial Engineering Department, Faculty of Engineering, Rajamangala University of Technology Krungthep, Thailand. The authors duly acknowledge the technical support of the University Laboratory, especially Piyapong Kumkoon and Kritsana Uamunson, who are lecturers who provide infrastructural facilities and technical support and share their experiences during the research.

#### References

- [1] P. Baras, J. Sawicki, Numerical analysis of mechanical properties of 3D printed aluminium components with variable core infill values, *Journal of Achievements in Materials and Manufacturing Engineering* 103/1 (2020) 16-24.  
DOI: <https://doi.org/10.5604/01.3001.0014.6912>
- [2] L. Kaczmarek, P. Kula, J. Sawicki, S. Armand, T. Castro, P. Kruszyński, A. Rochel, New possibilities of applications aluminium alloys in transport, *Archives of Metallurgy and Materials* 54/4 (2009) 1199-1205.
- [3] M. Fonte, M. Freitas, L. Reis, Failure analysis of a damaged diesel motor crankshaft, *Engineering Failure Analysis* 102 (2019) 1-6.  
DOI: <https://doi.org/10.1016/j.engfailanal.2019.04.025>
- [4] V. Infante, M. Freitas, M. Fonte, Failure analysis of a crankshaft of a helicopter engine, *Engineering Failure Analysis* 100 (2019) 49-59.  
DOI: <https://doi.org/10.1016/j.engfailanal.2019.01.072>
- [5] K. Aliakbari, R. Nejad, S. Toroq, W. Macek, R. Branco, Assessment of unusual failure in the crankshaft of



- heavy-duty truck engine, *Engineering Failure Analysis* 134 (2022) 106085.  
DOI: <https://doi.org/10.1016/j.engfailanal.2022.106085>
- [6] D. Kopeliovich, Knowledge source on materials engineering, Available from: [http://www.substech.com/dokuwiki/doku.php?id=engine\\_bearing\\_housing\\_and\\_how\\_it\\_affects\\_engine\\_bearings&s=misalignment](http://www.substech.com/dokuwiki/doku.php?id=engine_bearing_housing_and_how_it_affects_engine_bearings&s=misalignment), Access in: 15.06.2023.
- [7] Y. Zhang, G. Chen, L. Wang, Thermoelastohydrodynamic analysis of misaligned bearings with texture on journal surface under high-speed and heavy-load conditions, *Chinese Journal of Aeronautics* 32/5 (2019) 1331-1342.  
DOI: <https://doi.org/10.1016/j.cja.2018.08.005>
- [8] M. Lahmar, D. Frihi, D. Nicolas, The effect of misalignment on performance characteristics of engine main crankshaft bearings, *European Journal of Mechanics - A/Solids* 21/4 (2002) 703-714. DOI: [https://doi.org/10.1016/S0997-7538\(01\)01202-5](https://doi.org/10.1016/S0997-7538(01)01202-5)
- [9] B. Kareem, Evaluation of failures in mechanical crankshafts of automobile based on expert opinion, *Case Studies in Engineering Failure Analysis* 3 (2015) 25-33.  
DOI: <https://doi.org/10.1016/j.csefa.2014.11.001>
- [10] O. Hrevtsev, N. Selivanova, P. Popovych, L. Poberezhny, V. Ya. Brych, Yu. Rudyak, O. Shevchuk, N. Bakulina, R. Rozum, M. Buriak, Stress-strain state simulation of non-uniformly heated elements of components and assemblies of automotive, *Journal of Achievements in Materials and Manufacturing Engineering* 115/1 (2022) 26-32.  
DOI: <https://doi.org/10.5604/01.3001.0016.2339>
- [11] O. Hrevtsev, N. Selivanova, P. Popovych, L. Poberezhny, V. Sakhno, O. Shevchuk, L. Poberezhna, I. Murovanyi, A. Hrytsanchuk, O. Romanyshyn, Simulation of thermomechanical processes in disc brakes of wheeled vehicles, *Journal of Achievements in Materials and Manufacturing Engineering* 104/1 (2021) 11-20.  
DOI: <https://doi.org/10.5604/01.3001.0014.8482>
- [12] S. Baragetti, Design Criteria for High Power Engines Crankshafts, *The Open Mechanical Engineering Journal* 9 (2015) 271-281.  
DOI: <http://dx.doi.org/10.2174/1874155X01509010271>
- [13] P.G. Ikonov, A. Yahamed, P.D. Fleming, A. Pekarovicova, Design and testing 3D printed structures for bone replacements, *Journal of Achievements in Materials and Manufacturing Engineering* 101/2 (2020) 76-85. DOI: <https://doi.org/10.5604/01.3001.0014.4922>
- [14] T.P. Kersten, H.-J. Przybilla, M. Lindstaedt, Investigations of the Geometrical Accuracy of Handheld 3D Scanning Systems, *Photogrammetrie – Fernerkundung – Geoinformation* 5-6 (2016) 271-283.  
DOI: <http://dx.doi.org/10.1127/pfg/2016/0305>
- [15] Geomagic Software - Innovia3D, Workflow from 3D Scanning to Post-Processing, Available from: <https://www.innovia3d.com/products/geomagic-software>, Access in: 15.06.2023.
- [16] D. Redaelli, S. Barsanti, E. Biffi, F. Storm, G. Colombo, Comparison of geometrical accuracy of active devices for 3D orthopaedic reconstructions, *The International Journal of Advanced Manufacturing Technology* 114 (2021) 319-342.  
DOI: <https://doi.org/10.1007/s00170-021-06778-0>
- [17] G. Taubin, D. Moreno, 3D Scanning for Personal 3D Printing: Build Your Own Desktop 3D Scanner, Available from: <http://mesh.brown.edu/desktop3dscan>, Access in: 15.06.2023.
- [18] S. Raza, M. Amjad, K. Ishfaq, S. Ahmad, M. Abdollahian, Effect of Three-Dimensional (3D) Scanning Factors on Minimizing the Scanning Errors Using a White LED Light 3D Scanner, *Applied Sciences* 13/5 (2023) 3303.  
DOI: <https://doi.org/10.3390/app13053303>
- [19] W. Khuanglieng, R. Saodaen, P. Janmancee, Case Study of Broken Engine's Crankshaft Investigation, *Proceedings of the 8<sup>th</sup> Rajamangala Manufacturing and Management Technology Conference, Chonburi Province, 2023*, 782-790.
- [20] A. Khathri, M. Ismail, A. Abdullah, R. Mamat, S. Sutiman, Performance, Exhaust Emissions and Optimization Using Response Surface Methodology of a Water in Diesel Emulsion on Diesel Engine, *Journal of Advanced Research in Fluid Mechanics and Thermal Sciences* 93/1 (2022) 1-12.  
DOI: <https://doi.org/10.37934/arfm.93.1.112>
- [21] The HandySCAN 3D, Technical specifications, Available from: <https://www.creaform3d.com/en/handyscan-3d-silver-series-professional-3d/technical-specifications>, Access in: 15.06.2023.
- [22] R. Bonin, F. Khameneifar, J.R.R. Mayer, Evaluation of the Metrological Performance of a Handheld 3D Laser Scanner Using a Pseudo-3D Ball-Lattice Artifact, *Sensors* 21/6 (2021) 2137.  
DOI: <https://doi.org/10.3390/s21062137>
- [23] ProCarManuals, ISUZU Diesel engine, Workshop Repair Manual, Engine mechanical 4JK1/4JJ1 model 6A 129-132, Available from: <https://procarmanuals.com/pdf-online-isuzu-kb-p190-2007-iworkshop-repair-manual>, Access in: 20.01.2023.

- [24] M. Givi, L. Cournoyer, G. Reain, B. Eves, Performance evaluation of a portable 3D imaging system, *Precision Engineering* 59 (2019) 156-165. DOI: <https://doi.org/10.1016/j.precisioneng.2019.06.002>
- [25] M. Wiater, G. Chladek, J. Żmudzki, FEM numerical simulation of contact stresses between driving shaft and hub impeller of fuel pump, *Journal of Achievements in Materials and Manufacturing Engineering* 113/1 (2022) 13-21. DOI: <https://doi.org/10.5604/01.3001.0016.0941>
- [26] K. Khaeroman, G. Haryadi, R. Ismail, S. Kim, Failure analysis and evaluation of a six cylinders crankshaft for marine diesel generator, *AIP Conference Proceedings* 1788 (2017) 030064. DOI: <https://doi.org/10.1063/1.4968317>
- [27] T.P. Kersten, M. Lindstaedt, D. Starosta, Comparative geometrical accuracy investigation of hand-held 3D scanning systems-An update, *The International Archives of the Photogrammetry, Remote Sensing and Spatial Information Sciences XLII-2* (2018) 487-494. DOI: <https://doi.org/10.5194/isprs-archives-XLII-2-487-2018>
- [28] A. Jiao, B. Liu, X. Chen, X. Zou, F. Wang, Fracture Failure Analysis of KL Crankshaft, *Engineering Failure Analysis* 112 (2020) 104498. DOI: <https://doi.org/10.1016/j.engfailanal.2020.104498>
- [29] M. Nargolkar, Analysis of crankshaft, *International Journal of Scientific Engineering and Research* 5/4 (2017) 122-127.
- [30] F.J. Jiménez-Espadafor, J.A. Becerra Villanueva, M. Torres García, Analysis of a diesel generator crankshaft failure, *Engineering Failure Analysis* 16/7 (2009) 2333-2341. DOI: <https://doi.org/10.1016/j.engfailanal.2009.03.019>



© 2024 by the authors. Licensee International OCSCO World Press, Gliwice, Poland. This paper is an open-access paper distributed under the terms and conditions of the Creative Commons Attribution-NonCommercial-NoDerivatives 4.0 International (CC BY-NC-ND 4.0) license (<https://creativecommons.org/licenses/by-nc-nd/4.0/deed.en>).